Energy Landscape of the Tautomer States of Mesoporphyrin Embedded in Horseradish Peroxidase

Levente Herenyi,* Judit Fidy,* Jurgen Gafert,‡ and Josef Friedrich‡
*Institute of Biophysics, Semmelweis Medical University, Budapest, Hungary, and ‡ Physikalisches Institut und Bayreuther Institut für Makromolekulforschung, Universitat Bayreuth, Bayreuth, Germany

ABSTRACT The energy hypersurface of the dominant tautomer states of mesoporphyrin-substituted horseradish peroxidase was determined by creation of a nonequilibrium population of these states through photochemical transformation at 5 K and measurement of the temperature changes of the respective spectral bands as they were warmed to room temperature.

INTRODUCTION

The physical as well as the functional properties of proteins are determined through their respective energy landscapes. The problem is that for complex systems, such as proteins, the energy landscape is not accessible either experimentally or computationally. The situation is similar to that of spin glasses, but in detail it is more complicated because the responsible interactions are less well known. It is accepted that even small proteins have a huge number of conformational substates and that there are different hierarchy classes among these states (Ansari et al., 1985; Young and Bowne, 1984; Frauenfelder et al., 1988, 1991). A thoroughly investigated example is the so-called taxonomic states in myoglobin. These are conformational substates that are distinguished through their different CO stretch frequencies and the respective polarization directions. At sufficiently low temperatures these substates are separated by energy barriers. The next lower hierarchy level in the substates is manifested in the inhomogeneous line broadening of the respective IR bands and in a distribution of the associated CO coordination barriers. An even lower hierarchy level can be addressed in spectral diffusion experiments (Zollfrank et al., 1991).

Here we address the problem of the energy landscape of photochemically induced states of the porphyrin within a hemoprotein. The situation is similar to that for the taxonomic states. For example, if the chromophore is a free base porphyrin-type molecule, these photochemically induced states are the tautomer states related to the various configurations of the two inner-ring protons (Fidy et al., 1992; Gafert et al., 1993; Friedrich et al., 1994; Gafert et al., 1994a). Note that throughout this paper we use the term "configuration" only in the context of the tautomer states of the two inner-ring protons to stress the special nature of these states. Examples that have been studied based on this concept are mesoporphyrin-substituted horseradish peroxidase and protoporphyrin-substituted myoglobin (Gafert et al., 1994b; Gafert et al., 1993; Gafert et al., 1994c). It has been shown that the two inner-ring protons can arrange themselves in a series of configurations that form a complicated energy hypersurface. Some of these configurational states have rather high energies compared with physiological temperatures, so they are not or are only slightly populated at room temperature, but they can be photochemically populated at low temperatures; at 5 K all these states are totally isolated (Fidy et al., 1992). Spectral diffusion and isothermal compressibility measurements indicate that different tautomers of the chromophore correspond to distinct protein conformational distributions (Fidy et al., 1992; Friedrich et al., 1994; Gafert et al., 1994a).

In horseradish peroxidase (the protein on which we focus in this paper), the (0, 0) bands of the tautomeric configurations are spectrally well distinguishable. This was the basis of our experimental approach: We created a nonequilibrium population of the tautomer states and measured the temperature-dependent absorption spectra (more precisely the fluorescence excitation spectra) from which we extracted information on the energy landscape. The procedure yields the heights of the various configurational barriers (Kohler and Friedrich, 1987; Kohler et al., 1988; Berendzen and Braunstein, 1990) and, in principle, also the relative energies of these states. Generally, this latter information is not easily accessible because the total number of states and the temperature dependence of the respective transitions have to be known. The problem is that some of the states may be buried underneath the inhomogeneous width and are hard to identify. Thus it is also hard to determine their temperature dependence. In our case we can definitely identify four tautomer states, but there may be more. For each of three of them the associated temperature-dependent spectrum can be measured sufficiently accurately and an energy hypersurface can be determined.

EXPERIMENTAL

For the measurement, the native iron proto-heme of horseradish peroxidase (HRP) has been replaced by free-base

Received for publication 23 December 1994 and in final form 18 May 1995.

Address reprint requests to Dr. Judit Fidy, Institute for Biophysics, Semmelweis Medical University, H-1444 P.O.B. 263, Budapest, Hungary. Tel: 36-1-267-6261; Fax: 36-1-266-6656; E-mail: judit@puskin.sote.hu.

0006-3495/95/08/577/06 $2.00

mesoporphyrin (MP). It was shown earlier (Horie et al., 1985) that aromatic H donors bind to HRP with high affinity even when reconstituted with a metal-free porphyrin. Hence HRP still maintains its substrate binding ability even after MP substitution. HRP isoenzyme C2 has been isolated from horseradish roots and purified as described by Paul and Stigbrand (1970). The pure fraction was treated with 2-butanone (Teale, 1995), and the apoprotein was recombined with purified mesoporphyrin IX. Samples were prepared in 50-mM ammonium acetate, at 200 K and pH 5. The pH of the samples was changed to pH 8 by dialysis. 50% glycerol was added to ensure transparency; thus the final concentration of MP–HRP was 20 μM.

The sample was quickly frozen to low temperatures. The absorption spectrum taken at low temperature was practically not influenced by the cooling procedure. After photobleaching at 5 K, the samples were slowly warmed up. The experiments were carried out in a He flow cryostat.

The light source for photobleaching was an Ar-ion-laser-pumped ring dye laser with a bandwidth of the order of 10^{-4} cm^{-1}. It was scanned in a 1-wave-number range and tuned with a birefringent filter (by hand) through a large range of the inhomogeneous width of the B_1 and B_3 bands (Fig. 1, *a* and *b*). The power levels used for irradiation were in the milliwatt range.

The fluorescence excitation spectra were measured with a Jobin-Yvon THR 1000 monochromator whose resolution was set to ~5 cm^{-1}.

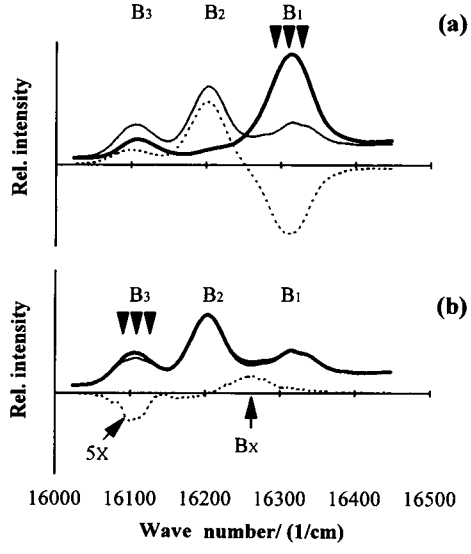

FIGURE 1 The fluorescence excitation spectra of MP–HRP at 5 K and the influence of photobleaching: the spectrum before irradiation (*thick curves*) and after irradiation (*thin curves*) and the difference spectrum (*dashed curves*). The wave-number range of the bleaching light is marked by arrow tips. The respective bands of the tautomer states are labeled B_1–B_3. (*a*) Photobleaching of B_1; (*b*) irradiation within B_3. Note that the spectrum shown by the thin curve in *a* belongs to the same state as that shown by the thick curve in *b*. The appearance of a new band B_x is shown by a magnified (5×) difference spectrum.

RESULTS

Fig. 1, *a* and *b* and Fig. 2 summarize the results of the whole series of experiments. In Fig. 1, *a* and *b* the fluorescence excitation spectra of MP–HRP are shown before and after photobleaching together with the respective difference spectra at 5 K. For convenience we have labeled the respective bands in an arbitrary fashion with B_1–B_3 (as we did earlier (Friedrich et al., 1994; Gafert et al., 1994a)), and we have also marked the wave-number range of photobleaching. The bands correspond with different tautomer states of MP.

As can be seen from the difference of the two spectra (dashed curve in Fig. 1 *a*) taken before and after photobleaching, the positive and negative areas are equal. This means that the intensity change of the bands depends on the population of the respective states only. In Fig. 1 *b* we show the effect of irradiation in B_3. Note the appearance of a new band, which we denote B_x. It is clearly seen in the magnified (5×) difference spectrum.

Fig. 2 shows a selected series of fluorescence excitation spectra while the temperature was increased after photobleaching of B_1. From these data we constructed the two-dimensional surface (Fig. 3 *a*), representing the relative intensity as a function of wave number and temperature. In this representation the appearance and disappearance of the various bands are clearly discernible.

The heights of the different bands as a function of temperature are represented in Fig. 3 *b*. The photobleached B_1 band does not change up to ~100K, but then it suddenly increases, runs through a maximum, and slowly decreases. The B_2 band practically decreases in two steps. The first step occurs near 25 K, the second one near 100 K. The B_3 band also changes in two steps: it first increases near 25 K and decreases near 100 K.

To produce temperature-derivative signals we subtracted successive fluorescence excitation spectra from each other

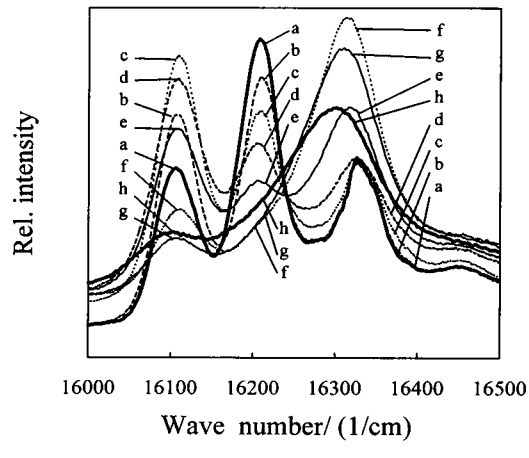

FIGURE 2 Selected series of fluorescence excitation spectra of MP–HRP as a function of temperature after photobleaching of the B_1 band at 5 K. The respective temperatures are represented by different line types, marked by different letters: *a*, 10 K; *b*, 30 K; *c*, 50 K; *d*, 90 K; *e*, 100 K; *f*, 110 K; *g*, 140 K; *h*, 180 K.

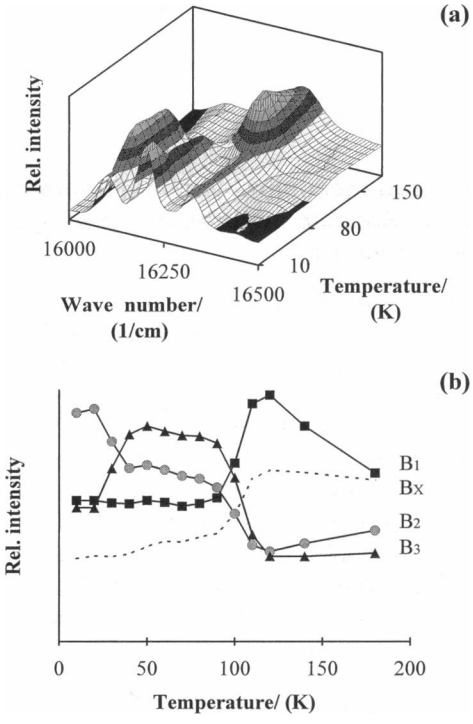

FIGURE 3 (*a*) Relative intensities of the fluorescence excitation spectra of MP–HRP as a function of wave number and temperature represented as a two-dimensional surface. (*b*) The heights of the various bands as a function of temperature: a one-dimensional cross section of the surface shown in (*a*) along the typical wave numbers of the respective maxima.

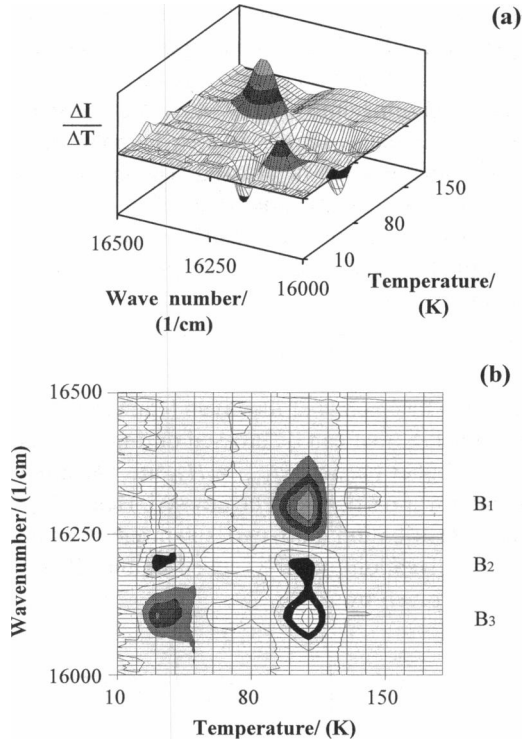

FIGURE 4 The temperature derivative spectrum of MP–HRP. The successive fluorescence excitation spectra were subtracted from each other and divided by ΔT, and the $\Delta I/\Delta T$ signals are represented as a function of wave number and temperature. (*a*) Two-dimensional surface representation, (*b*) contour map representation. Note that the same gray-tone representation is used in both (*a*) and (*b*). The distribution of barrier heights can be determined by a cut through the surface in (*a*) along the typical wave number of the respective maximum.

and divided by ΔT. Fig. 4 *a* and *b* represents the temperature-derivative spectrum (Berendzen and Braunstein, 1990) as a two-dimensional surface (Fig. 4 *a*) and as a contour map (Fig. 4 *b*). The height is represented by a gray-tone scale both in the negative and in the positive directions. By this method, the distribution of barrier height(s) of the respective energy landscape is mapped.

DISCUSSION

Basic concepts of the experimental procedure

After the protein is cooled to 5 K, it is the B_1 state that is strongly populated and that carries almost all the total intensity of the S_1–S_0 transition (Fig. 1 *a*). Some population is also trapped in the B_3 state (a small band can be seen in the spectrum at the respective frequency range). In the experiment the B_1 state was heavily bleached, at 5 K, by broadband photochemistry. As a consequence, states B_2 and B_3 got populated, and an additional state B_x of very low population could be identified by the magnified (5×) difference spectrum (Fig. 1 *b*). We stress that the photochemically induced population is a nonequilibrium population that is stable at 5 K, because the respective states are separated by sufficiently large barriers.

The spectrum is given by the intensity function

$$I(\bar{\nu}) = \sum_n p_n I_n(\bar{\nu} - \bar{\nu}_n), \qquad (1)$$

where p_n is the population probability of the photochemically created state B_n. I_n is the intensity of the respective inhomogeneously broadened absorption band, centered at $\bar{\nu}_n$. At this point we introduce the specific features of our system to simplify Eq. 1. From Fig. 1 *a* it is clear that the photochemistry in B_1 does not change the overall intensity: what is missing in band B_1 appears in the other bands (B_2, B_3). The conclusion is that I_n does not depend strongly on the specific state *n*. Hence it is a constant and can be put in front of the summation sign. In other words, the configurational changes of the inner-ring protons do not significantly affect the oscillator strength.

The temperature dependence of the spectrum is determined through the temperature dependence of the population probabilities p_n. p_n depends on two parameters, namely, the height of the barrier (H_{nm}) that separates state B_n from state B_m and the respective energy (E_n). The barrier height determines the respective relaxation kinetics, whereas the energy determines the stationary populations after equilibrium is reached.

Suppose that the kinetics is governed by activated processes with a rate

$$R_{nm} = R_0 \exp(-H_{nm}/k_B T) \qquad (2)$$

and that there is a rather broad distribution of activation enthalpies (P_H). The initial, nonequilibrium population in state n is assumed to be at higher energy than in state m. Then, at a certain temperature, when the thermal energy approaches the range of the barrier heights, part of the activation enthalpies can be crossed. The intensity originating from state n decreases, and that of m increases. For a given temperature there is a specific barrier H_M (M stands for "marginal") in the distribution P_H. It is determined through the condition

$$R_{nm}(H_M) = 1/\tau. \tag{3}$$

Equation 3 means that at the given temperature H_M is the maximum height that can be crossed during the experimental time τ. Higher barriers $H_{nm} > H_M$ are essentially unaffected, but lower barriers will be crossed. Hence H_M divides the whole distribution into two subensembles: in subensemble I, relaxation occurs; subensemble II is frozen. Hence, p_n is given by

$$p_n(T) = f_n \int_0^{H_M} P_H \, dH + \int_{H_M}^{\infty} P_H \, dH, \tag{4}$$

with H_M determined by Eqs. 2 and 3:

$$H_M = k_B T \ln(R_0 \tau). \tag{5}$$

The factor f_n accounts for the fact that state n can be repopulated from m. If the states involved reach equilibrium, f_n is given by

$$f_n = \frac{\exp(-E_n/k_B T)}{\sum_N \exp(-E_n/k_B T)}. \tag{6}$$

N is the number of states involved in the equilibrium. There are two interesting cases to be considered, namely, those limits for which f_n is temperature independent. This is the case when $E_n \gg k_B T$ and $E_n \ll k_B T$. In the first case f_n is close to zero; in the second case it is close to $1/N$. Thus, in the first case, the first term in Eq. 4 vanishes; in the other case both terms play a role. The important aspect, however, is that in either case the derivative of p_n, and, hence according to Eq. 1 the derivative of the measured intensity with respect to temperature, yields the distribution of barrier heights P_H over a temperature scale. Fig. 4 *a* shows the derivative functions, and Fig. 4 *b* is a projection of Fig. 4 *a* onto a temperature–wave-number plane (Berendzen and Braunstein, 1990). Contour maps as obtained from temperature-derivative signals provide insight into the conformational hierarchy. They were used to explain details of the light-induced relaxation effect in myoglobin (Nienhaus et al., 1994).

There are two points that need to be emphasized: (1) According to Eq. 5, temperature and barrier height are proportional. From the experimental results, the barrier height is given on a temperature scale. (2) The barriers that we measure are "one sided," i.e., they are the barriers seen from the upper state.

Application to mesoporphyrin in horseradish peroxidase. Specific features of the temperature-dependent spectrum

We discuss the specific features of the temperature-dependent spectrum by considering the temperature-dependent intensities in the three bands at fixed frequencies; i.e., we consider three cuts through the surface in Fig. 3 *a* along frequencies $\nu_{B1} = 16\,320\ cm^{-1}$, $\nu_{B2} = 16\,203\ cm^{-1}$, and $\nu_{B3} = 16\,108\ cm^{-1}$ (Fig. 3 *b*) (the exact band parameters were determined by Smeller's software (Smeller et al., 1994)). The respective intensities at 5 K are determined by the degree of photobleaching. Above 20 K, barrier crossing between states B_2 and B_3 becomes possible. Near 45 K, both states reach a steady state–like intensity plateau. The temperature range where the intensity decrease of B_2 and the intensity increase of B_3 occurs is determined through the width of the respective distribution of barriers H_{23}, which separates state B_2 from B_3. This width is ~25 K and is of the same order of magnitude as the average height, which is 30 K.

From the measured intensity pattern as a function of temperature it is obvious that state B_3 is lower in energy than B_2. As a consequence, barrier $H_{32} > H_{23}$. Hence equilibrium between the subensemble of communicating states is not immediately established. As the temperature surpasses the higher barriers of the distribution, equilibrium will be reached, and, as a consequence, the intensities of the two states enter a plateau regime between 45 and 90 K. In this range the intensity of the B_1 band stays constant. Hence it is obvious that B_2 and B_3 are decoupled from B_1 up to ~90 K. From the stationary intensity regime we can determine the energy difference between B_2 and B_3: it is approximately 7–9 cm^{-1}.

There is a subtle feature to be addressed: Although the population of B_1 is unchanged, there is a slight decrease of the population in B_2 and B_3 in the plateau range. We interpret this phenomenon as an indication of the presence of a fourth state. Indeed, there is such a state, as can be seen in Fig. 1 *b*, where the magnification of the difference spectrum reveals this B_x band at a frequency of 16 261 cm^{-1} in the close neighborhood of the B_1 band. A cut through the energy surface along the respective frequency is shown in Fig. 3 *b* by a dashed curve.

Near 100 K the intensity of the B_1 state increases strongly at the expense of bands B_2 and B_3. Again the temperature range between 90 and 120 K, where the B_1 band increases, is determined by the distribution of barriers H_{m1} ($m = 2, 3$). The width σ_H of this distribution is ~30 K, and its maximum is centered at 100 K. Again the average barrier height is comparable with the width of the distribution. Beyond 130 K the intensity of B_1 decreases. We interpret this as a

repopulation process of B_2, B_3, and B_x that becomes effective above this temperature. Hence the intensity decay characterizes the establishment of equilibrium among the various states. From the decay into equilibrium we can determine the absolute energies of B_2 and B_3 with respect to B_1. Because we measured the barriers as well, we can reconstruct a cut through the energy hypersurface on an absolute scale (in units of kelvins). This is done in Fig. 5.

At this point we note that, whereas the temperatures for the valleys in Fig. 5 are determined from equilibrium conditions (and, thus, k_BT converts them into an energy scale), the temperatures for the barriers are determined from kinetic relations (Eq. 2). Hence, in the latter case, k_BT has to be scaled with the factor $\ln(R_0\tau)$ (see Eq. 5) to yield the correct energy scale. One possible solution to this problem is to estimate the scaling factor from a reasonable guess for the preexponential factor R_0. Because of the logarithmic dependence it is only the order of magnitude that counts (Kohler and Friedrich, 1987; Kohler et al., 1989a, 1989b). Another approach would be to estimate the absolute scale from nuclear magnetic resonance or fluorescence experiments (Abraham et al., 1974; Storm and Teklu, 1972; Butenhoff and Moore, 1988). The estimates of the barrier heights from these experiments, which probed two diagonal proton configurations only, amount to a few thousand wave numbers. This is in a reasonable accordance with a preexponential rate factor R_0 of the order of 10^{12} s^{-1}. We stress the order-of-magnitude character of these numbers. Yet they show that the barriers can be very high compared with to the ground-state energy differences of the respective tautomers (see also the previous section).

As of yet, the exact structures of the tautomeric states have not been identified, but it is clear that there are tautomer-specific interactions between apoprotein and inner-ring protons. For instance, it has been shown that the protein changes global parameters, such as its compressibility, when the chromophore is switched from one tautomer to another (Gafert et al., 1994a). Resonance Raman spectroscopy, which is a powerful method for studying porphyrin structures within native hemoproteins (Powers et al., 1987), would be the straightforward technique to elucidate the tautomer configurations and to provide details of the respective interactions with the protein. However, the efficient phototransformation processes in free base porphyrins together with a strong fluorescence emission seem to hamper a straightforward application of Q_x band resonance Raman techniques. (In the Soret or in the Q_y band the tautomers cannot be spectrally resolved.) Moreover, for HRP the x-ray structure is not known. Hence at present it is impossible to correlate the specific features of the energy hypersurface, as determined in our experiment, with specific structural details of the apoprotein.

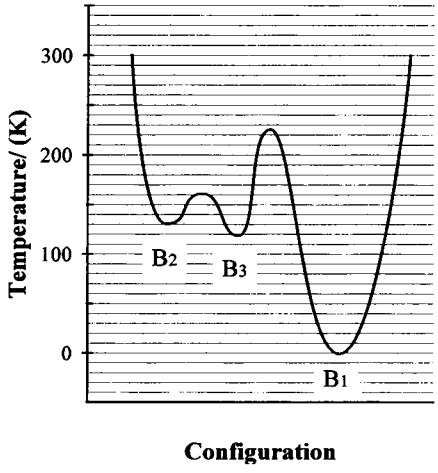

FIGURE 5 One-dimensional cross section of the energy hypersurface (energy landscape) of the dominant tautomer states of MP–HRP on a relative temperature scale. The mean temperatures for the valleys are determined from equilibrium condition; hence k_BT is the equivalent energy scale. The mean temperatures for the barriers are determined from the distribution of barrier heights; hence k_BT has to be scaled by the factor $\ln(R_0\tau)$ to yield the correct energy scale.

Aspects of disorder: distribution of barriers and inhomogeneous line broadening

In a spatially strictly correlated ensemble of molecules, we would expect well-defined barriers and energies. The fact that barriers and energies are distributed in proteins reflects the fact that the arrangement of the molecular building blocks in a protein is not perfectly correlated. From the order of magnitude of the widths of the respective distributions, one infers that the degree of spatial correlation in proteins is between those of crystals and glasses, yet closer to the behavior of a glass (Gafert et al., 1994a, 1994b). Inhomogeneous distributions of barriers and absorption energies reflect the subconformations of the apoprotein: for a given tautomer state the apoprotein can exist in many subconformations, each of which generates a specific energy surface for the tautomer. Along these lines of reasoning, barrier distribution and inhomogeneous line broadening have the same origin. In principle one should be able to determine the scaling factor between temperatures and energies (see Eq. 5) from a comparison between the width of the barrier distribution and the inhomogeneous width of the absorption bands. In our case a typical inhomogeneous bandwidth is 100 cm^{-1}, corresponding to 144 K, and a typical width of the barrier distribution is 30 K. Based on these data and Eq. 5, one would infer that the scaling factor $\ln(R_0\tau)$ is of the order of 5. One may estimate the experimental time equal to ~10 s, and thus the preexponential would be of the order of 15 s^{-1}. This is, however, orders of magnitudes too low. There may be two reasons why this scaling between inhomogeneous line broadening and barrier distribution does not work: (1) A strong (energetic) correlation between the energy hypersurface in the electronic ground and excited states. This could narrow the optical lines tremendously. That this kind of energetic correlation between S_1 and S_0 does exist has been shown in several

investigations (Flach et al., 1977; Griesser and Wild, 1980; Sevian and Skinner, 1992; Lee et al., 1985). (2) Inhomogeneous line broadening scales with the temperature where the system falls out of equilibrium ("the glass transition temperature"). Above this temperature the conformational substates are in equilibrium. The barrier states, on the other hand, are never in equilibrium; hence their energies can, in principle, vary on quite different scales, as the order-of-magnitude estimates from nuclear magnetic resonance and fluorescence experiments show.

We argue that these two reasons, namely, energetic correlation and the partial equilibrium nature of the conformational substates involved in inhomogeneous line broadening, are responsible for the absence of a common scale between barrier distribution and inhomogeneous line broadening.

SUMMARY

Mesoporphyrin in horseradish peroxidase shows a series of tautomeric states that differ in their inner-ring proton configurations. These states, of which we could spectroscopically identify four, communicate with one another on a very complicated energy hypersurface, giving rise to a complex temperature dependence of the absorption spectrum. From this temperature dependence we could reconstruct the energy surface in a frequency–temperature parameter space. This energy surface reflects the structural disorder of the protein, which leads to the broad distributions of the configurational enthalpic barriers.

We acknowledge support from the DFG (SFB 213-B15, Graduiertenkolleg "Nichtlineare Dynamik") (J.Fr.), from the Fonds der Chemischen Industrie, from the BMFT (WTZ-program Germany–Hungary) (J.Fr. and J.Fi.), and Hungarian grants FEFA 265 and 693 (J.Fi.).

REFERENCES

Abraham, R. J., G. E. Hawkes, and K. M. Smith. 1974. N–H tautomerism in porphyrins: an NMR study. *Tetrahedron Lett.* 16:1483–1486.

Ansari, A., J. Berendzen, S. F. Bowne, H. Frauenfelder, I. E. T. Iben, T. B. Sauke, E. Shyamsunder, and R. D. Young. 1985. Protein states and proteinquakes. *Proc. Natl. Acad. Sci. USA.* 82:5000–5004.

Berendzen, J., and D. Braunstein. 1990. Temperature-derivative spectroscopy: A tool for protein dynamics. *Proc. Natl. Acad. Sci. USA.* 87:1–5.

Butenhoff, T. J., and C. B. Moore. 1988. Hydrogen atom tunneling in the thermal tautomerism of porphin imbedded in an *n*-hexane matrix. *J. Am. Chem. Soc.* 110:8336–8341.

Fidy, J., J. M. Vanderkooi, J. Zollfrank, and J. Friedrich. 1992. More than two pyrrole tautomers of mesoporphyrin stabilized by a protein. *Biophys. J.* 61:381–391.

Flach, R., D. S. Hamilton, P. M. Selzer, and W. M. Yen. 1977. Laser induced fluorescence line narrowing studies of impurity ion systems: $LaF_3:Pr^{3+}$. *Phys. Rev. B.* 15:1248–1260.

Frauenfelder, H., F. Parak, and B. Young. 1988. Conformational substates in proteins. *Ann. Rev. Biophys. Chem.* 17:451–479.

Frauenfelder, H., S. G. Sligar, and P. G. Wolynes. 1991. The energy landscapes and motions of proteins. *Science.* 254:1598–1603.

Friedrich, J., J. Gafert, J. Zollfrank, J. M. Vanderkooi, and J. Fidy. 1994. Spectral hole burning and selection of conformational substates in chromoproteins. *Proc. Natl. Acad. Sci. USA.* 91:1029–1033.

Gafert, J., J. Friedrich, and F. Parak. 1993. A comparative pressure tuning hole burning study of protoporphyrin IX in myoglobin and in a glassy host. *J. Chem. Phys.* 99:2478–2486.

Gafert, J., J. Friedrich, J. M. Vanderkooi, and J. Fidy. 1994a. Correlation between protein conformation and prosthetic group configuration as tested by pH-effects: A hole-burning study on mesoporphyrin-IX-substituted horseradish peroxidase. *J. Phys. Chem.* 98:2210–2214.

Gafert, J., C. Ober, K. Orth, and J. Friedrich. 1994b. A comparative hole burning study of thermal line broadening in proteins and glasses. *J. Chem. Phys.* In press.

Gafert, J., J. Friedrich, and F. Parak. 1994c. Stark-effect experiments on photochemical holes in chromoproteins: protoporphyrin-IX substituted myoglobin. *Proc. Natl. Acad. Sci.* USA. In press.

Griesser, H. J., and U. P. Wild. 1980. Energy selection experiments in glassy matrices: the line width of the emissions $S_2 \rightarrow S_0$ and $S_2 \rightarrow S_1$ of azulene. *J. Chem. Phys.* 73:4715–4719.

Horie, T., J. M. Vanderkooi, and K.-G. Paul. 1985. Study of the active site of horseradish peroxidase isoenzymes A and C by luminescence. *Biochemistry.* 24:7931–7936.

Kohler, W., and J. Friedrich. 1987. Distribution of barrier heights in amorphous organic materials. *Phys. Rev. Lett.* 59:2199–2202.

Kohler, W., J. Friedrich, and H. Scheer. 1988. Conformational barriers in low temperature proteins and glasses. *Phys. Rev. A.* 37:660–662.

Kohler, W., J. Zollfrank, and J. Friedrich. 1989a. Thermal irreversibility in optically labelled low-temperature glasses. *Phys. Rev. B.* 39:5414–5423.

Kohler, W., J. Zollfrank, and J. Friedrich. 1989b. Stability of frequency domain information bits in amorphous organic materials. *J. Appl. Phys.* 66:3232–3240.

Lee, H. W. H., C. A. Walsh, and M. D. Fayer. 1985. Inhomogeneous broadening of electronic transitions of chromophores in crystals and glasses: analysis of hole burning and fluorescence line narrowing experiments. *J. Chem. Phys.* 82:3948–3958.

Nienhaus, G. U., J. R. Mourant, K. Chu, and H. Frauenfelder. 1994. Ligand binding to heme proteins: the effect of light to ligand binding in myoglobin. *Biochemistry.* 33:13413–13430.

Paul, K.-G., and T. Stigbrand. 1970. Four isoperoxidases from horseradish root. *Acta. Chem. Scand.* 24:3607–3617.

Powers, L., B. Chance, M. Chance, B. Campbell, J. Friedman, S. Khalid, C. Kumar, A. Naqui, K. S. Reddy, and Y. Zhou. 1987. Kinetic, structural, and spectroscopic identification of geminate states of myoglobin: a ligand binding site on the reaction pathway. *Biochemistry.* 26: 4785–4796.

Sevian, H. M., and J. L. Skinner. 1992. A molecular theory of inhomogeneous broadening, including the correlation between different transitions, in liquids and glasses. *Theor. Chim. Acta.* 82:29–46.

Smeller, L., K. Goossens, and K. Heremans. 1994. How to avoid artifacts in Fourier self-deconvolution. *Appl. Spectrosc.* In press.

Storm, C. B., and Y. Teklu. 1972. Nitrogen-hydrogen tautomerism in porphyrins and chlorins. *J. Am. Chem. Soc.* 94:1745–1747.

Teale, F. W. J. 1959. Cleavage of the hemoprotein link by acid methyl ethyl ketone. *Biochim. Biophys. Acta.* 35:543.

Young, R. D., and S. F. Bowne. 1984. Conformational substates and barrier height distributions in ligand binding to heme proteins. *J. Chem. Phys.* 81:3730–3737.

Zollfrank, J., J. Friedrich, J. M. Vanderkooi, and J. Fidy. 1991. Proteins and glasses: a comparative study of spectral diffusion phenomena. *J. Chem. Phys.* 95:3134–3136.